

AUGER ELECTRON SPECTROSCOPIC STUDY OF THE CN ANION: A STUDY OF THE NaCN(001) SURFACE IN COMPARISON WITH CO AND N₂

H. PULM, C.-M. LIEGENER¹ and H.-J. FREUND

*Institut für Physikalische und Theoretische Chemie der Universität Erlangen–Nürnberg,
Egerlandstrasse 3 8520 Erlangen, Federal Republic of Germany*

Received 15 May 1985, in final form 18 June 1985

We have recorded the carbon and nitrogen KVV Auger spectra of NaCN, excited with X-rays. The spectra are interpreted on the basis of *ab initio* many-body calculations of the double hole state energies and intensities of CN⁻. The nitrogen (KVV) Auger spectrum of NaCN is more similar to the N(KVV) spectrum of N₂ than the carbon (KVV) Auger spectrum of NaCN is to the C(KVV) spectrum of CO. This observation is well reproduced by the calculations. We conclude that the strong influence of the localization of the orbitals in CO on the Auger spectra has disappeared in CN⁻, although the delocalization is not as pronounced as in N₂. On the basis of the calculations it is possible to assign satellite structure in the N(KVV) Auger spectrum of CN⁻, in comparison to the N(KVV) Auger spectrum of N₂.

1. Introduction

Recently, we reported a detailed study of photoelectron spectra taken on a solid NaCN(001) surface [1]. It was possible to show that the photoemission from the surface was completely determined by photoemission from the CN⁻ sublattice of the crystal. The energetically lowest detectable Na ionisation was the Na 2p ionisation about 26.5 eV below the lowest observed vertical ionisation potential, consistent with almost complete charge separation into Na⁺ and CN⁻. Using theoretical *ab initio* many-body calculations on the CN anion photoelectron spectrum, we were able to assign the complete outer and inner valence photoelectron spectrum including shake-up satellites.

The results presented in this Letter extend the former study to Auger spectra. We report X-ray induced spectra of a NaCN(001) surface and analyse the spectra

- (i) by comparison with the N(KVV) Auger spectrum of N₂ [2] and the C(KVV) Auger spectrum of CO [2],
- (ii) by comparison with *ab initio* many-body calculations of the CN⁻ Auger spectra using a Green's func-

tion approach as developed by Liegener [3] and previously applied to CO [4] and N₂ [5].

CN⁻, which is isoelectronic with CO and N₂, has unlike N₂, but like CO, two core–valence–valence (KVV) spectra, termed C(KVV) and N(KVV). Both spectra represent the same final states, which means that the lines have the same relative energy positions with respect to the corresponding core ionisations (N 1s and C 1s) but quite different intensity distributions. We show that the N(KVV) spectrum of CN⁻ is in general more comparable to the N(KVV) Auger spectrum of N₂ than the CN⁻ C(KVV) Auger spectrum to the C(KVV) spectrum of CO, and that this trend is well reproduced by the calculations. Our comparison between experimental and theoretical results clearly indicates that the dramatic influence of the strong localization of the orbitals in CO on the Auger spectra has disappeared in CN⁻, although the orbital delocalization in CN⁻ is not as pronounced as in N₂.

However, a detailed comparison between the N(KVV) spectra of N₂ and CN⁻ reveals differences in peak positions and intensities that can be rationalized on the basis of qualitative arguments about the valence electron wavefunctions. The most obvious difference is the absence of a pronounced shake-up-induced band in the CN⁻ spectrum as compared to N₂. An ex-

¹ Lehrstuhl für Theoretische Chemie der Universität Erlangen–Nürnberg

planation of this observation can be given on the basis of our theoretical results.

2. Experimental procedure

The spectra were recorded using a modified Leybold-Heraeus LHS 10 photoelectron spectrometer. As an excitation source we used an $\text{AlK}\alpha$ X-ray anode. The spectra were taken with 256 data points per scan and a dwell time of 2 s per point. About 200 scans were averaged for the spectra shown in figs. 1 and 2. The base pressure in the instrument was 10^{-10} Torr. There was no observable change in the $\text{N}(\text{KVV})$ spectrum

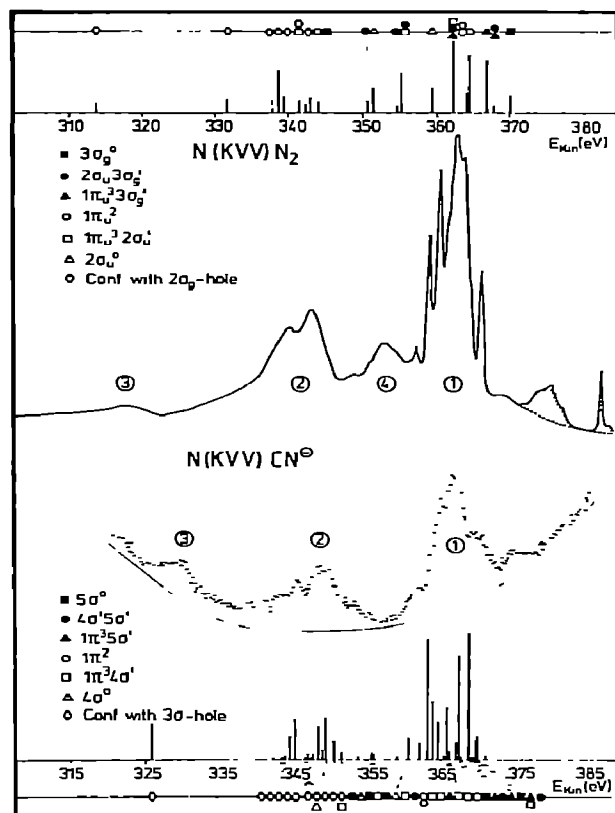


Fig. 1. Comparison of the $\text{N}(\text{KVV})$ Auger spectra of NaCN (dotted trace) and of N_2 [2] (full line). The energy scales refer to the experimental spectra. Theoretical results are given as line spectra. The dominant double-hole state configurations are indicated (for details see table 2).

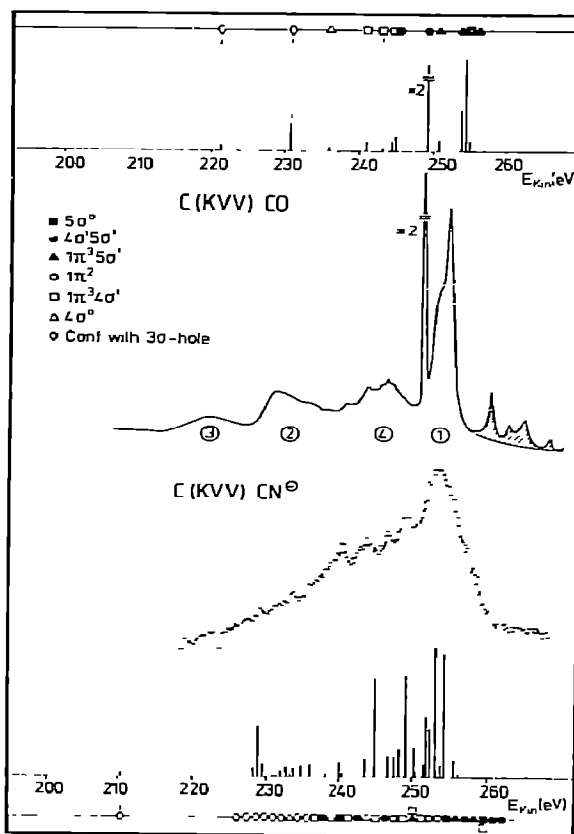


Fig. 2. Comparison of the $\text{C}(\text{KVV})$ Auger spectra of NaCN (dotted trace) and of CO [2] (full line). The energy scales refer to the experimental spectra. Theoretical results are given as line spectra. The dominant double-hole state configurations are indicated (for details see table 2).

even after recording the spectra for 48 h. The $\text{C}(\text{KVV})$ spectrum was relatively sensitive to the presence of carbon containing contamination. The sample of highly purified NaCN was pressed into metallic indium in order to contact it to the sample holder. Kinetic energies are referred to literature values of metallic indium. The results are presented in comparison to the corresponding spectra of N_2 and CO and the theoretical results in figs. 1 and 2. The shapes of the background signals of the CN spectra are indicated. The curved background shape for the $\text{N}(\text{KVV})$ CN^- spectrum is due to photoionisation of $\text{Na } 1s$ electrons in NaCN. The measured kinetic energies of the main features of

Table 1
Observed features in NaCN Auger spectra (E_{kin} (eV))

| N(KVV) | | C(KVV) | |
|----------|----------|----------|----------|
| relative | absolute | relative | absolute |
| 0.0 | 375.0 | 0.0 | 252.2 |
| 4.9 | 370.1 | 9.8 | 242.4 |
| 8.0 | 367.0 | 20.8 | 231.4 |
| 9.6 | 365.4 | 26.4 | 225.8 |
| 26.2 | 348.8 | | |
| 29.5 | 345.5 | | |
| 46.6 | 328.4 | | |

the CN^- spectra are collected in table 1.

The Auger spectra included in figs. 1 and 2 for comparison have been taken from the work of Moddeman et al. [2] and are excited by electron impact. The lines for which we have evidence that they are caused by de-excitation via ionization of a K-electron excited state [2,6] are indicated as hatched areas. Those lines are not observed in a photon-induced spectrum if the photon energy is sufficiently high.

3. Theoretical procedure

The method used has been described in detail elsewhere and we refer to the literature [3–5] for reference. The present method has the pronounced advantage over other methods used to calculate Auger spectra that it remains valid also in cases where the quasiparticle picture for some of the single-ionization processes breaks down. Within the calculational scheme the double ionization potentials ($\text{DIP} = E_{\text{kin}} - \text{IP}$; IP = ionization potential for the initial-state core hole), corresponding to the final states of the Auger transitions are calculated as zeros of the eigenvalues of the inverse particle–particle Green's matrix:

$$\mathbf{G}^{-1}(\omega) = \mathbf{G}^{(0)-1}(\omega) - \mathbf{K}, \quad (1)$$

where \mathbf{K} is the first-order irreducible vertex part and

$$G_{klmn}^{(0)}(\omega) = \sum_{\mu\nu} \gamma_{k\mu\nu} P_{k\mu} P_{l\nu} \delta_{km} \delta_{ln} / (\omega - \omega_{k\mu} - \omega_{l\nu}), \quad (2)$$

where $\omega_{k\mu}$ are the poles of the one-particle Green's function in the diagonal approximation and $P_{k\mu}$ are

the corresponding pole strengths[‡]. Furthermore, $\gamma_{k\mu\nu} = -1$ if both $\omega_{k\mu}$ and $\omega_{l\nu}$ are negative, $\gamma_{k\mu\nu} = 1$ if both are positive, and $\gamma_{k\mu\nu} = 0$ otherwise. For the (KVV) spectra $\omega_{k\mu}$ and $P_{k\mu}$ contain the information of the valence-electron photoelectron spectrum. The sum over μ (ν) covers the poles into which the single-particle ionization, with energy $-\epsilon_k$, is split by turning on electron correlation. The indices refer to Hartree–Fock ground-state data on CN^- . Only poles with $P_{k\mu}$ greater than certain threshold values (see below) were included, thus ensuring that $\omega_{k\mu} < 0$ if k belongs to the set of occupied orbitals, and $\omega_{k\mu} > 0$ if k belongs to the set of unoccupied orbitals. The transition rates (TR) for the various final states were estimated by modulating the matrix elements (evaluated within the one-center model) with the corresponding residues of the one-particle Green's function. The Hartree–Fock data used as input for the calculation of the Auger spectra of CN^- were calculated with the aid of a double zeta Gaussian basis set [1] using the experimental geometry [8]. The $\omega_{k\mu}$ and $P_{k\mu}$ were taken from the extended two-particle–hole (2ph) Tamm–Dancoff calculations reported earlier [1]. The core orbitals and the virtual orbitals above the 7σ orbital of CN^- were not renormalized. The integrals involving continuum wavefunctions were obtained employing the radial integrals of McGuire [9]. Two sets of calculations were performed in order to evaluate the influence of the shake-up structure of the valence ionization spectrum on the (KVV) Auger spectra. A similar approach was chosen earlier by Liegener [5] to study satellite effects in the N_2 Auger spectrum. In the first of the present calculations the threshold for the $P_{k\mu}$ was set to 0.055, thus excluding all poles due to outer-valence shake-up, i.e. shake-up satellites borrowing their intensity out of the outer-valence orbitals, 4σ , 1π and 5σ [7,10,11] while still including inner-valence shake-up structure associated with the 3σ ionization. In the second calculation all poles $\omega_{k\mu}$ [1] were included, i.e. the threshold for the $P_{k\mu}$ was set to 0.005. We show the results of the latter calculation in table 2. Line spectra representing the results of table 2 are included in figs. 1 and 2 for comparison with the experimental spectra. The line spectra for CO and N_2 are taken from refs.

[‡] For reviews on one-particle Green's function methods see ref. [7].

Table 2
Auger spectra of CN^- , calculated with the first-order irreducible vertex part (energies in eV, TRs in arbitrary units)

| Symmetry | DIP a) | TR(C) | TR(N) | Dominant components b) |
|--------------|--------------|-------|-------|--|
| $^3\Sigma^+$ | 16.22(-0.19) | 0.021 | — | $4\sigma^1 5\sigma^1$ (0.99) |
| $^1\Sigma^+$ | 16.59(-0.08) | 0.177 | 0.073 | $4\sigma^1 5\sigma^1$ (0.47), $5\sigma^0$ (0.35), $4\sigma^0$ (0.17) |
| $^3\Pi$ | 17.79(-0.23) | — | 0.065 | $1\pi^3 5\sigma^1$ (0.59), $4\sigma^1 1\pi^3$ (0.41) |
| $^1\Pi$ | 17.98(-0.07) | 0.019 | 0.301 | $4\sigma^1 1\pi^3$ (0.68), $1\pi^3 5\sigma^1$ (0.32) |
| $^1\Sigma^+$ | 18.10(-0.66) | 1.166 | 0.309 | $5\sigma^0$ (0.62), $4\sigma^0$ (0.26), $4\sigma^1 5\sigma^1$ (0.11) |
| $^3\Pi$ | 18.51(-0.61) | 0.120 | 0.042 | $1\pi^3 5\sigma^1$ (0.99) |
| $^3\Sigma^+$ | 18.97(-0.62) | 0.070 | 0.027 | $4\sigma^1 5\sigma^1$ (0.99) |
| $^1\Pi$ | 19.29(-0.68) | 1.227 | 1.897 | $1\pi^3 5\sigma^1$ (0.96) |
| $^1\Sigma^+$ | 20.11(-0.21) | 0.464 | 0.033 | $5\sigma^0$ (0.78) |
| $^1\Delta$ | 20.50(-0.60) | 0.590 | 1.551 | $1\pi^2$ (0.99) |
| $^1\Sigma^+$ | 20.85(-0.49) | 0.134 | 0.243 | $1\pi^2$ (0.97) |
| $^3\Pi$ | 21.77(-0.31) | 0.056 | 0.114 | $4\sigma^1 1\pi^3$ (0.99) |
| $^1\Pi$ | 22.12(-0.17) | 0.099 | 0.760 | $1\pi^3 5\sigma^1$ (0.58), $4\sigma^1 1\pi^3$ (0.42) |
| $^3\Pi$ | 22.39(-0.37) | 0.172 | 0.041 | $4\sigma^1 1\pi^3$ (0.63), $1\pi^3 5\sigma^1$ (0.37) |
| $^1\Pi$ | 23.33(-0.50) | 0.980 | 0.546 | $4\sigma^1 1\pi^3$ (0.81), $1\pi^3 5\sigma^1$ (0.19) |
| $^1\Delta$ | 24.08(-0.25) | 0.243 | 0.640 | $1\pi^2$ (1.00) |
| $^1\Sigma^+$ | 24.11(-0.34) | 0.031 | 0.239 | $1\pi^2$ (0.59), $5\sigma^0$ (0.17), $4\sigma^1 5\sigma^1$ (0.15) |
| $^1\Sigma^+$ | 24.72(-0.64) | 0.199 | 1.717 | $4\sigma^1 5\sigma^0$ (0.56), $5\sigma^0$ (0.30) |
| $^3\Pi$ | 25.48(-0.07) | 0.020 | 0.020 | $4\sigma^1 1\pi^3$ (0.97) |
| $^1\Pi$ | 25.69(-0.15) | 0.199 | 0.294 | $4\sigma^1 1\pi^3$ (0.95) |
| $^1\Sigma^+$ | 27.27(-0.41) | 0.947 | 0.356 | $4\sigma^0$ (0.66), $5\sigma^0$ (0.15), $4\sigma^1 5\sigma^1$ (0.12) |
| $^1\Sigma^+$ | 28.72(-0.08) | 0.187 | 0.041 | $4\sigma^1 5\sigma^1$ (0.77), $4\sigma^0$ (0.20) |
| $^1\Pi$ | 31.88(-0.03) | 0.033 | 0.082 | $4\sigma^1 1\pi^3$ (0.99) |
| $^1\Sigma^+$ | 32.23(-0.07) | 0.151 | 0.084 | $5\sigma^0$ (0.64), $4\sigma^0$ (0.33) |
| $^1\Sigma^+$ | 34.08(-0.03) | 0.030 | 0.026 | $4\sigma^0$ (0.73), $3\sigma^1 5\sigma^1$ (0.11) |
| $^1\Sigma^+$ | 36.31(-0.07) | 0.131 | 0.092 | $4\sigma^1 5\sigma^1$ (0.94) |
| $^3\Pi$ | 37.24(-0.04) | 0.010 | 0.013 | $4\sigma^1 1\pi^3$ (1.00) |
| $^1\Pi$ | 37.34(-0.05) | 0.052 | 0.137 | $4\sigma^1 1\pi^3$ (0.99) |
| $^3\Sigma^+$ | 37.63(-0.66) | 0.053 | 0.148 | $3\sigma^1 5\sigma^1$ (0.96) |
| $^1\Sigma^+$ | 38.58(-0.36) | 0.092 | 0.613 | $3\sigma^1 5\sigma^1$ (0.85), $3\sigma^1 4\sigma^1$ (0.11) |
| $^3\Pi$ | 38.99(-0.55) | 0.028 | 0.161 | $3\sigma^1 1\pi^3$ (0.99) |
| $^1\Sigma^+$ | 39.64(-0.03) | — | 0.076 | $3\sigma^1 4\sigma^1$ (0.56), $4\sigma^0$ (0.40) |
| $^1\Sigma^+$ | 39.89(-0.07) | 0.042 | 0.220 | $4\sigma^0$ (0.43), $3\sigma^1 4\sigma^1$ (0.34), $3\sigma^1 5\sigma^1$ (0.20) |
| $^1\Sigma^+$ | 39.97(-0.07) | 0.061 | 0.212 | $4\sigma^0$ (0.43), $3\sigma^1 5\sigma^1$ (0.33), $3\sigma^1 4\sigma^1$ (0.22) |
| $^1\Sigma^+$ | 40.13(-0.01) | 0.021 | 0.036 | $3\sigma^1 5\sigma^1$ (0.52), $4\sigma^0$ (0.40) |
| $^1\Pi$ | 40.34(-0.02) | — | 0.032 | $3\sigma^1 1\pi^3$ (1.00) |
| $^1\Sigma^+$ | 40.44(-0.03) | 0.048 | 0.037 | $3\sigma^1 1\pi^3$ (0.67), $4\sigma^0$ (0.30) |
| $^1\Pi$ | 40.83(-0.05) | 0.020 | 0.082 | $3\sigma^1 1\pi^3$ (1.00) |
| $^3\Sigma^+$ | 41.32(-0.25) | 0.017 | 0.033 | $3\sigma^1 4\sigma^1$ (0.94) |
| $^1\Pi$ | 42.69(-0.35) | 0.137 | 0.577 | $3\sigma^1 1\pi^3$ (1.00) |
| $^1\Pi$ | 43.09(-0.07) | 0.028 | 0.120 | $3\sigma^1 1\pi^3$ (1.00) |
| $^1\Sigma^+$ | 43.14(-0.03) | 0.037 | 0.014 | $3\sigma^1 4\sigma^1$ (0.76), $3\sigma^1 5\sigma^1$ (0.17) |
| $^1\Sigma^+$ | 43.41(-0.30) | 0.423 | 0.194 | $3\sigma^1 4\sigma^1$ (0.77), $3\sigma^1 5\sigma^1$ (0.18) |
| $^1\Sigma^+$ | 44.03(-0.06) | 0.079 | 0.055 | $3\sigma^1 4\sigma^1$ (0.84), $3\sigma^1 5\sigma^1$ (0.12) |
| $^1\Pi$ | 44.44(-0.02) | — | 0.025 | $3\sigma^1 1\pi^3$ (1.00) |
| $^1\Pi$ | 45.60(-0.02) | — | 0.028 | $3\sigma^1 1\pi^3$ (1.00) |
| $^1\Sigma^+$ | 62.18(-0.60) | 0.047 | 0.540 | $3\sigma^0$ (0.97) |

a) Pole strengths in parentheses. b) Squares of the eigenvector components in parentheses.

[4,5] and represent results of calculations of comparable quality.

4. Discussion

As mentioned in section 1, the valence electron photoemission of the NaCN surface is determined exclusively by the CN anion sublattice [1]. Therefore, we expect that the (KVV) Auger decay leads to double-hole states localized on the CN anion sublattice when the primary core hole is of C 1s or N 1s character. Since the CN⁻ sublattice behaves like a molecular solid with relatively weak intermolecular valence interactions (the Coulomb interaction between anions is screened by the Na⁺ ions), the Auger spectra should reflect the properties of the individual CN anions. Consequently, we compare the CN⁻ Auger spectra with Auger spectra of isoelectronic molecular gases, namely N₂ and CO. In addition we assign the spectra on the basis of many-body *ab initio* calculations of the (KVV) double-hole state energies and Auger transition rates of CN⁻.

Let us first discuss the N(KVV) spectrum of CN⁻ as shown in the lower part of fig. 1. The lower kinetic-energy scale refers to the experimental spectrum. The spectrum consists of three band systems, separated by broad minima. The most intense system at highest kinetic energies has been aligned with the most intense band system of the N(KVV) spectrum of N₂ [2] shown in the upper part of fig. 1. There have been several calculations on the doubly ionized state energies of N₂ [5,12–14] providing a qualitative understanding of the Auger spectrum of N₂. (However, an unambiguous one-to-one assignment of the close lying sharp lines in the high-energy region seems not to be possible at present.) The most intense structure ((1) in fig. 1) at high kinetic energies is due to double-hole states with both holes in the outer-valence region. The region ((2) in fig. 1) at lower kinetic energy has been assigned to double-hole states where there is one hole in the inner-valence region, while the band ((3) in fig. 1) at lowest kinetic energy is due to an inner-valence double-hole state. An inspection of fig. 1 suggests that this qualitative assignment can be directly transposed to the CN⁻ spectrum. Our calculations, in addition, support this as is indicated by the symbols below the theoretical line spectrum. For all (or the most intense)

lines the main double-hole configuration from which most of the intensity of the line is borrowed is indicated. The distribution of one double-hole-state configuration over several lines is caused by the presence of shake-up structure in the single-hole-state (photoelectron) spectrum. In other words, the existence of satellite lines in the photoelectron spectrum leads to the appearance of extra lines in the Auger spectrum. In the calculations the energies and intensities of the double-hole states sensitively depend on those details of the single-hole-state spectrum. The N(KVV) Auger spectrum of N₂ is a case where this has been demonstrated theoretically [5]. The feature (4) in fig. 1 in this spectrum is reproduced by the calculations only if shake-up satellites on the outer-valence electrons are included. Such an extra structure is not observed in the CN⁻ spectrum at comparable energetic position. In order to study the influence of satellite structure on the CN Auger spectra we performed calculations where we neglected outer-valence shake-up. The result is very similar to the full calculation, especially with respect to the qualitative structure of regions (1), (2) and (3). However, the results indicate that the shoulder at high kinetic energy of region (2) is caused by coupling to outer-valence shake-up although the effect is much less pronounced than in N₂.

The relative intensities of the three spectral regions are correctly predicted by the calculations. In fact, most of the details in the spectrum are predicted by the calculations in a semiquantitative way: Region (1) has a shoulder at high kinetic energies (assigned to states derived from parent configurations involving $4\sigma^1 5\sigma^1$, $1\pi^3 5\sigma^1$ and $5\sigma^0$), a peak with three or four not completely resolved main components (parent configurations involved are $1\pi^3 5\sigma^1$, $1\pi^2$, $4\sigma^1 1\pi^3$ and $4\sigma^1 5\sigma^1$), and a shoulder at low kinetic energies (parent configurations $4\sigma^1 1\pi^3$ and $4\sigma^0$). The most intense lines in region (1) correspond to states with parent configurations $4\sigma^1 5\sigma^1$, $1\pi^2$, $1\pi^3 5\sigma^1$ and $1\pi^3 4\sigma^1$, while $5\sigma^0$ and $4\sigma^0$ do not seem to contribute as much to the intensity. This is in correspondence with the results for N₂. Region (2) consists of at least three peaks and shoulders at both high- and low-kinetic-energy side. This region is made up mainly of lines involving one 3σ hole (parent configurations $3\sigma^1 5\sigma^1$, $3\sigma^1 1\pi^3$ and $3\sigma^1 4\sigma^1$), but also some satellites with parent configuration $4\sigma^1 1\pi^3$ and $4\sigma^0$ contribute to this region. Region (3), finally, consists of a single broad peak, cor-

responding to the $3\sigma^0$ double-hole state. The relative energy position of peak (3) in the CN^- spectrum is shifted by about 6.5 eV to higher kinetic energy with respect to the N_2 spectrum while the positions of regions (1) and (2) approximately line up. In fact, the shift of peak (3) could have been expected after considering the differences of relative ionization energies of CN^- and N_2 as reported in ref. [1]:

While the relative ionization energies (with respect to the 4σ ionization) for outer-valence ionizations in CN^- are only ≈ 0.5 eV lower than those in N_2 , the inner-valence 3σ ionization is by ≈ 3 eV lower in CN^- than in N_2 . Peak (3), which is in both, N_2 and CN^- spectrum, assigned to the inner-valence double-hole state ($3\sigma^0$) will, therefore, shift to relatively higher kinetic energies in CN^- .

We now turn to the discussion of the C(KVV) spectrum of CN^- as shown in fig. 2. The kinetic-energy scale at the bottom refers to the experimental spectrum. The peak of highest intensity has been aligned with the C(KVV) spectrum of CO which is included in fig. 2 for comparison. The spectrum is less structured than the N(KVV) spectrum of fig. 1 and the comparison with the CO C(KVV) spectrum seems to be much less adequate ^{‡‡}. This, however, is exactly the prediction of the calculations. The number of lines expected for the CN^- spectrum is by a factor of 3 higher than for the CO spectrum. There are at least two possible reasons for this behaviour:

- (i) the influence of satellite lines,
- (ii) the loss of localization of the wavefunctions in CN^- as compared to CO.

Again, a calculation where the shake-up structure is artificially excluded shows that the effect of outer-valence shake-up is minor in this case, analogously to our findings for the N(KVV) spectrum of CN^- . We, therefore, conclude that (ii), i.e. the loss of localization, is operative. This result is in agreement with our calculations on the wavefunction of CN^- and with earlier calculations by several authors [16–20]. Even though CN^- is like CO in having no centre of inversion, the wavefunctions look more like those of N_2 than those of CO.

^{‡‡} Several theoretical calculations of the C(KVV) spectrum of CO have been reported. See for example refs. [4,15].

4. Conclusions

We have presented C(KVV) Auger spectra of the NaCN(001) surface. Comparisons with the C(KVV) spectrum of CO and the N(KVV) spectrum of N_2 and with results of theoretical ab initio many-body calculations support our previous conclusion [1] that the spectra are indicative of the CN anion sublattice only. The theoretical calculations allow for a rather detailed interpretation of the Auger spectra including satellite structure. We conclude that the CN anion valence-electron wavefunctions are more delocalized than the CO valence-electron wavefunctions, and that this causes the pronounced similarity of the N(KVV) spectrum of CN^- to the spectrum of N_2 .

Acknowledgement

We would like to thank Professor Dr. G. Hohlneicher for providing the LHS 10 XP spectrometer, and Professor Dr. W. von Niessen for kindly making available the computer printouts of ref. [1]. We are particularly grateful to Professor Dr. S. Haussühl for providing the NaCN single crystal. HJF thanks the "Fonds der Chemischen Industrie" for financial support.

References

- [1] H. Pulm, B. Marquardt, H.-J. Freund, R. Engelhardt, K. Seki, U. Karlsson, E.F. Koch and W. von Niessen, *Chem. Phys.* 92 (1985) 457.
- [2] W.E. Moddeman, T.A. Carlson, H.O. Krause, B.P. Pullen, W.E. Bull and G.K. Schweitzer, *J. Chem. Phys.* 55 (1971) 2317.
- [3] C.-M. Liegener, *Chem. Phys. Letters* 90 (1982) 188; *Phys. Rev. A* 23 (1983) 256; *Chem. Phys.* 92 (1985) 97.
- [4] C.-M. Liegener, *Chem. Phys. Letters* 106 (1984) 201.
- [5] C.-M. Liegener, *J. Phys.* B16 (1983) 4281.
- [6] C.T. Chen, W.K. Ford, L.W. Plummer, W. Eberhardt, R.P. Messmer and H.-J. Freund, submitted for publication.
- [7] L.S. Cederbaum and W. Domcke, *Advan. Chem. Phys.* 36 (1977) 36; J. Schürmer and O. Walter, *Chem. Phys.* 78 (1982) 201.
- [8] J.M. Brigvoet and J.A. Lely, *Rec. Trav. Chim.* 59 (1940) 908.
- [9] E.J. McGuire, *Phys. Rev.* 185 (1969) 1.
- [10] W. Eberhardt and H.-J. Freund, *J. Chem. Phys.* 78 (1983) 700.

- [11] S. Krumacher, V. Schmidt and F. Wuilleumier, *J. Phys.* B13 (1980) 3993;
S. Krumacher, V. Schmidt, F. Wuilleumier, J.M. Bizeau and D. Ederer, *J. Phys.* B16 (1983) 1733.
- [12] S. Fraga and B.J. Ransil, *J. Chem. Phys.* 35 (1961) 669.
- [13] E.W. Thulstrup and A. Andersen, *J. Phys.* B8 (1975) 965.
- [14] H. Agren, *J. Chem. Phys.* 75 (1981) 1267.
- [15] I.H. Hillier and J. Kendrick, *Mol. Phys.* 31 (1976) 849,
H. Agren and H. Siegbahn, *Chem. Phys. Letters* 72 (1980) 498;
D.R. Jennison, J.A. Kelber and R.R. Rye, *Chem. Phys. Letters* 72 (1981) 604;
J.A. Kelber, D.R. Jennison and R.R. Rye, *J. Chem. Phys.* 75 (1981) 652;
C. Desmukh and R.G. Hayes, *Chem. Phys. Letters* 88 (1982) 384;
G.E. Laramore, *Phys. Rev. A*29 (1984) 23;
N. Correia, A. Flores and H. Agren, unpublished;
R. Manne and A. Agren, *Chem. Phys.* 93 (1985) 201.
- [16] R. Bonaccorsi, C. Petrongolo, E. Scrocco and J. Tomasi, *J. Chem. Phys.* 48 (1968) 1500.
- [17] E. Clementi and D. Klint, *J. Chem. Phys.* 50 (1969) 4899.
- [18] J.B. Moffat and H.E. Popkie, *J. Mol. Structure* 6 (1970) 155.
- [19] K.M. Griffing and J. Simons, *J. Chem. Phys.* 64 (1976) 3610.
- [20] P.R. Taylor, G.B. Bacskay, N.S. Hush and A.C. Hurky, *J. Chem. Phys.* 70 (1979) 448.